

Schottky Barriers and Coulomb Blockade in Self-Assembled Carbon Nanotube FETs

L. Marty,[†] V. Bouchiat,^{*,‡} C. Naud,[†] M. Chaumont,[†] T. Fournier,[‡] and A. M. Bonnot[†]

Laboratoire des Propriétés Electroniques des Solides and Centre de Recherches sur les Très Basses Températures, CNRS, BP166 X, F-38042 Grenoble Cedex 9, France

Received May 5, 2003

ABSTRACT

We report low-temperature electronic transport in batch-processed single-walled carbon nanotube (SWNT) field-effect transistors (FETs). SWNTs are in situ synthesized and wired between submicrometer metallic electrodes in a single-step process involving hot-filament-assisted chemical vapor deposition. FETs show a pronounced ambipolar field effect between 1 and 300 K. Moreover, the gate dependence exhibits hysteresis at any temperature because of the extraction and trapping of charges. We find Schottky barriers at the SWNT/metal contact to be responsible for the field effect. Below 30 K, potential barriers along the SWNT induce a Coulomb blockade at low drain-source bias, leading to the suppression of the field-effect gain and inducing fluctuations in the transconductance.

Single-walled carbon nanotubes (SWNTs) appear to be the most promising material to bridge the gap between top-down nanoelectronics and the emerging field of molecular electronics.¹ Nanometer-scale devices based on carbon nanotubes take advantage of their quasi-ideal 1D behavior combined with their metallic or semiconducting properties. Semiconducting SWNTs were integrated as a nanometer-sized channel in the early carbon nanotube field-effect transistors (CNFETs).² When optimizing the gate coupling, CNFETs exhibit a sufficient reproducibility and high enough gain to act as active components in integrated circuits performing a digital function³ that even exceed⁴ the best performance obtained by state-of-the-art silicon MOSFETs. Recently, a comprehensive analysis of CNFETs has shown evidence that the field effect originates from Schottky barriers at the metal/SWNT contacts.^{5,6}

This property brings to the fore the metal/SWNT interface and its necessary chemical and geometrical control.⁵ However, in most cases, implementing this connection involves difficult and time-consuming alignment or manipulation steps.⁷ Alternative methods are based on bottom-up techniques. They involve either in-situ growth by CVD methods^{8–10,4} or chemical self-assembly.¹¹ They enable batch processing and provide the scalability required to open the way to practical applications.¹²

In a similar approach, we have developed a self-assembling growth technique based on the hot-filament-assisted CVD technique¹³ (HFCVD). This batch process allows the growth of self-assembled SWNTs that are suspended and electrically wired between prepatterned metallic pads that act as nucleation sites.⁹ Raman spectroscopy as well as ex-situ transmission electron microscopy analysis confirm the high quality of our SWNTs with an average diameter of 1.2 nm.¹⁴ In the present work, samples consist of a few suspended bundles connecting titanium electrodes separated by a 300-nm gap (SEM micrograph in Figure 4, inset). The high surface temperature during the deposition ensures the formation of titanium carbide at the molecular interface,¹⁵ a feature that is expected to reduce the contact resistance.¹⁶ To investigate the reproducibility and the reliability of our self-assembled circuits, we have measured electron transport properties of as-grown samples without any postgrowth treatment. We expect our SWNTs to be free of defects induced by postprocesses¹⁷ such as sonication or chemical purification. We present here the first low-*T* electrical characterization of in-situ connected self-assembled CNFETs.

Electrical characterizations were conducted between 1 and 300 K using both DC measurements and a low-frequency lock-in detection technique. The gate was obtained by biasing the 0.5- μm -thick silica-covered Si substrate.

For all samples, drain-source *I*–*V* curves are always found to be linear at room temperature up to a 1 V drain-source bias with two-wire resistances ranging from 10 to 500 k Ω depending on the SWNT density and HFCVD parameters,

* Corresponding author. E-mail: bouchiat@grenoble.cnrs.fr.

[†] Laboratoire des Propriétés Electroniques des Solides.

[‡] Centre de Recherches sur les Très Basses Températures.

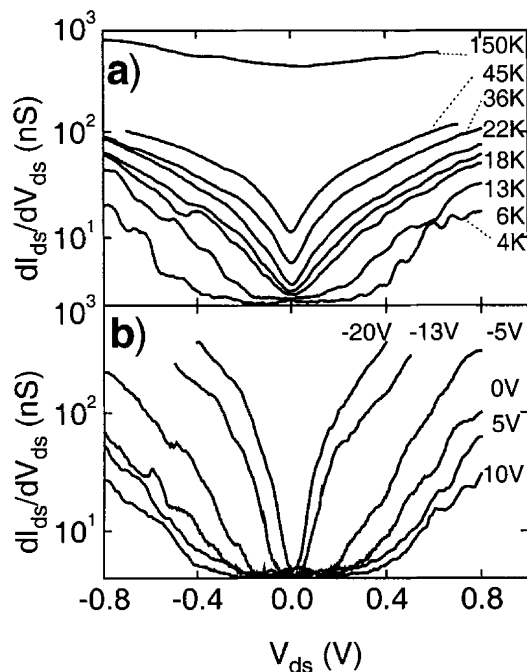


Figure 1. (a) Differential conductance vs drain-source voltage of a typical self-assembled CNFET for different temperatures (device in the off state). (b) Differential conductance vs drain-source voltage at 4 K for different gate voltages.

whereas they show increasing nonlinearity with decreasing temperature (Figure 1a). At 50 K, the current is a quadratic function of the voltage, and at 4 K, all samples exhibit a zero conductance gap with a sample-dependent width varying between 30 and 600 meV.

Whatever the temperature, a field effect is observed for 80% of the more than 50 tested samples. Raman microspectroscopy¹⁴ confirms the abundance of semiconducting SWNTs similarly to CNFETs obtained using other CVD methods.⁵

The field-effect amplitude is found to be strongly sample-dependent. It is characterized by the on-off current ratio $(I_{\text{on}}/I_{\text{off}})_{V_g}$, where I_{on} and I_{off} are drain-source currents measured respectively at gate voltages $\pm V_g$. $(I_{\text{on}}/I_{\text{off}})_{V_g}$ can be as low as 1.25 possibly because some metallic SWNTs may shunt the semiconducting SWNTs,¹⁹ and on other samples it can reach up to 10^4 at room temperature and 10^6 at low temperature (Figure 2). The field effect in our typical self-assembled CNFETs is mainly p type with an n-type contribution that less pronounced than the p type contribution. Such an ambipolar effect was seen essentially on CNFETs made of postprocessed SWNTs for which oxygen adsorbed on the SWNTs was removed by annealing^{15,19} after wiring. Because strong p doping is usually expected for air-exposed CNFETs, we attribute this difference to the CVD synthesis method, which is performed in a reductive^{9,20} atmosphere of atomic hydrogen that might passivate SWNTs.

Moreover, the drain-source current (Figure 2) depends on the sweep direction of the gate voltage. It clearly shows a hysteresis that is attributed to stored charges in interface traps close to the conducting SWNTs and has already been observed by several groups on CNFETs involving ex-situ-grown SWNTs^{21–24} and multiple-walled carbon nanotubes²⁵

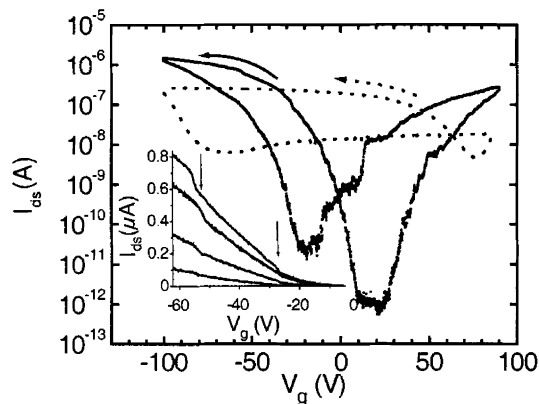


Figure 2. Gate dependence of the drain-source current at different temperatures and biases (dotted line $T = 300$ K, $V_{\text{ds}} = 50$ mV; solid line $T = 1$ K, $V_{\text{ds}} = +1$ V, sweep rate = 0.05 V·s⁻¹). Arrows indicate the hysteresis loop direction. Inset: Enlargement of hysteresis curves at 1 K for different drain-source voltages—top to bottom 1 V, 900 mV, 700 mV, and 500 mV. Current discrete steps at $V_g = -27$ and -55 V are indicated by arrows.

The gate-induced electric field is maximized in the SWNT vicinity because of the field-line concentration. It is on the order of 1 V/nm, which is over the breakdown field of SiO₂²⁶ (25 mV/nm) and thus strong enough for a field extraction of charges. These trapped charges are responsible for the observed hysteresis in the gate dependence of the transconductance.^{21–25} The hysteresis loop direction confirms^{23,27} that for positive gate voltages electrons are extracted from the SWNTs into the traps whereas holes are trapped for negative gate voltages. Additional features such as reproducible discrete steps occurring at regularly spaced gate voltages²⁵ are seen at low temperatures (inset of Figure 2). We believe that they are the signature of charge transfer involving a small number of charge quanta, a feature that usually occurs in single-electron memories^{28,29} and has been seen in carbon nanotube FETs.²⁵

Figure 1 depicts the drain-source voltage dependence of the differential conductance at different temperatures and at different gate voltages of a typical low-resistance sample. Whereas at high temperature the I - V curve is linear and conductance reaches $9 \mu\text{S}$ in the on state, a large zero-conductance gap of about 600 meV opens below 30 K (Figure 1a). This gap can be removed almost totally by applying a gate voltage, but a zero-conductance dip subsists at zero bias at 4 K even for high backgate voltages (Figure 1b). It must be noted that the respective influences of the gate voltage and the temperature on the differential conductance below 30 K give comparable effects. This suggests a transport limited by barriers that can be overcome either by thermal activation or by electrostatic doping. The physical origins of barriers limiting transport in CNFET are numerous: they can be induced by Schottky contacts at the metal/SWNT interface or by dopants (oxygen, water) adsorbed along the SWNT or even by intrinsic defects within the SWNT carbon lattice.^{30,31} A closer study of transport properties is required to allow the separation of competing phenomena that control electron transport in these CNFETs.

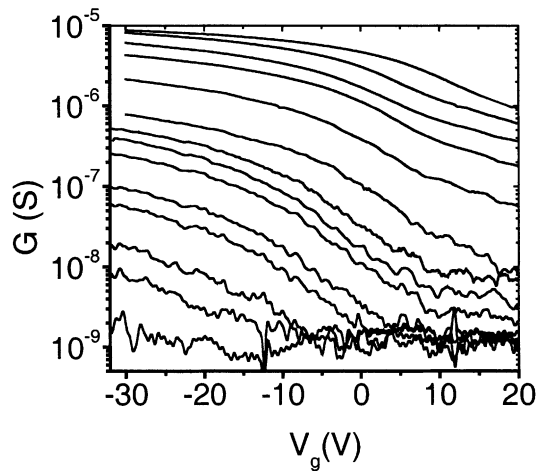


Figure 3. Gate dependence of the AC conductance at different temperatures (AC bias $V_{ds} = 5$ mV). Gate sweep rate = $-0.1 \text{ V}\cdot\text{s}^{-1}$ (from top to bottom: 275, 245, 200, 155, 100, 60, 54, 45, 39, 24, 17, 8, 6, 4K).

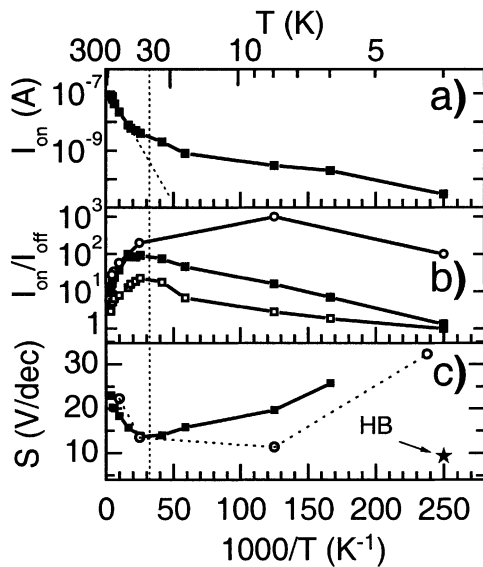


Figure 4. (a) Arrhenius plot of the drain-source DC current in the on state taken at $V_g = -30$ V, $V_{ds} = 10$ mV. (b) Arrhenius plot of the on-off ratio for increasing gate sweeps (bottom to top): $V_g = \pm 10, \pm 30, \pm 80$ V. (c) Temperature dependence of the subthreshold swing $S = dV_g/d \log I_{ds}$ measured for different drain-source voltages: (■) $V_{ds} = 5$ mV, (○) $V_{ds} = 100$ mV, (★) HB (high bias) $V_{ds} = 400$ mV.

An Arrhenius plot of the T dependence of the drain-source current in the on state (I_{on}) for hole accumulation is presented in Figure 4a. Thermally activated behavior is found between 50 and 300 K, a result that is a priori consistent with a thermoionic emission above the Schottky barriers. However, the resulting barrier height is 16 meV, which is 20 times smaller than the work function estimated for titanium/SWNT with a Fermi level pinned at mid-gap.¹⁵ An explanation invoked to explain a similar discrepancy obtained on titanium-contacted CNFETs¹⁵ is the peculiar behavior of 1D Schottky barrier contacts. The effective barrier height results from thermally assisted tunneling through a barrier with a logarithmic tail.⁴ Another feature in agreement with this theory is the linear I - V curve that is always found at 300 K.

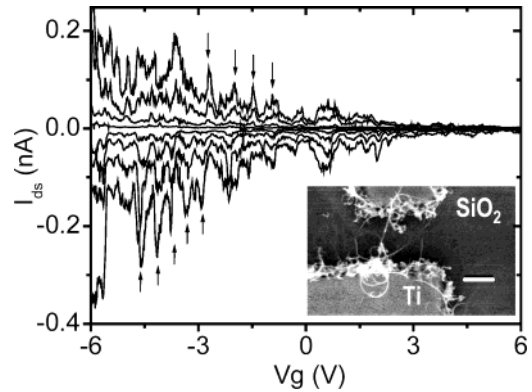


Figure 5. DC-measured gate dependence of the drain-source current at 4.2 K (bias voltage varying from +10 to -11 mV with -3 -mV steps). Inset: Scanning electron micrograph of a typical sample showing SWNT bundles bridging titanium electrodes. Scale bar is 200 nm.

As the temperature is lowered below 30 K, aperiodic fluctuations appear in the gate dependence of the drain-source current around the threshold voltage (Figure 5). Conductance peaks are clearly correlated between traces taken at different drain-source biases and exhibit a local periodicity of ~ 400 mV (arrows). They feature a Coulomb blockade in a disordered medium. Indeed, a single-island model cannot explain the complexity³² of the conductance peaks or such a wide gap. A single-electron transistor involving the whole SWNT length³³ would lead to a periodic oscillation of $e/C_g \approx 10$ mV where C_g is the SWNT backgate capacitance, which equals 15 aF in our case.

Similar features are commonly observed in silicon nanowires for which potential variations along the channel arises from "islands" in series created by a random distribution of dopants.^{34,35} Transport at low T and at low drain-source bias features the percolation of current through a multiple-tunnel-junction array.³⁶ It must be noted that similar barrier variations have been imaged by electrostatic scanning-probe microscopy at room temperature,³⁶ and their effect on transport has been probed by low- T scanning gate microscopy.³¹

The junctions in series thus enlarge the effective Coulomb gap.^{34,37} Because their number can vary considerably from sample to sample, this explains the wide dispersion of the measured Coulomb gaps.

Lowering the temperature reveals barriers along the SWNT channel, and below 30 K, electron transport is dominated by a Coulomb blockade at low drain-source biases. This leads to the partial suppression of the field effect created by the Schottky barriers at the SWNT/metal contacts (Figure 3). Such an effect makes our definitions of I_{on} and I_{off} deviate from that of real saturation currents. The temperature dependence of $(I_{on}/I_{off})_{V_g}$ for an increasing range of gate sweeps is depicted in Figure 4b. The wider the sweep range of the gate voltage $\pm V_g$, the larger the measured $(I_{on}/I_{off})_{V_g}$. But whatever the sweep range, (I_{on}/I_{off}) always exhibits a decrease with cooling that occurs at lower temperature for wider sweep ranges. This confirms the competition at low drain-source biases between the Schottky effect that domi-

nates transport at high temperature and the Coulomb blockade that partially suppresses the transconductance gain.

The evolution of the gate swing $S = dV_g/d \log I_{ds}$ with T measured at low drain-source bias ($V_{ds} = 5$ mV) is presented Figure 4c. It confirms the existence of a crossover at low drain-source bias between the two conduction regimes symbolized by a vertical dotted line. Above 30 K, S decreases with T whereas a sharp increase in S is observed below 30 K. However, if one looks at the field effect at a higher drain-source voltage ($V_{ds} = 100$ mV, open circles in Figure 4c), the increase in S is manifested at lower temperature. Furthermore, beyond the Coulomb gap, a strong field effect is still present at the lowest temperature (Figure 2b). Evaluating the subthreshold swing S at 4 K and at high bias gives a value comparable with S measured at 50 K (highlighted “HB” data in Figure 4c). This result is consistent with the low- T saturation of S expected in Schottky barrier FETs (SBFET) and observed in CNFETs.⁷

In conclusion, we have measured an ambipolar field effect on self-assembled in-situ-grown CNFETs. The hysteretical gate dependence of the drain-source current shows the strong interaction between the SWNTs and their local environment. The temperature dependence of all transport properties in our CNFETs is consistent with the presence of Schottky barriers at the contacts. However, at low drain-source bias and below 30 K, the SBFET behavior is concealed by a Coulomb blockade created by barriers scattered along the SWNT channel.

References

- (1) *Carbon Nanotubes*; Dresselhaus, M. S., Dresselhaus G., Avouris, Ph., Eds.; Springer: Berlin, 2001; Vol. 80.
- (2) Tans, S. J.; Verschuere, A. R. M.; Dekker, C. *Nature* **1998**, *393*, 49–52. Martel, R.; Schmidt, T.; Shea, H. R.; Hertel, T.; Avouris, Ph. *Appl. Phys. Lett.* **1998**, *73*, 2447–2449.
- (3) Bachtold, A.; Hadley, P.; Nakanishi, T.; Dekker, C. *Science* **2001**, *294*, 1317. Javey, A.; Wang, Q.; Ural, A.; Li, Y.; Dai, H. *Nano Lett.* **2002**, *2*, 929–932. Derycke, V.; Martel, R.; Appenzeller, J.; Avouris, Ph. *Nano Lett.* **2001**, *1*, 453–456.
- (4) Javey, A.; Kim, H.; Brink, M.; Wang, Q.; Ural, A.; Guo, J.; McIntyre, P.; McEuen, P.; Lundstrom, M.; Dai, H. *Nat. Mater.* **2002**, *1*, 241.
- (5) Heinze, S.; Tersoff, J.; Martel, R.; Derycke, V.; Appenzeller, J.; Avouris, Ph. *Phys. Rev. Lett.* **2002**, *89*, 106801.
- (6) Appenzeller, J.; Knoch, J.; Derycke, V.; Martel, R.; Wind, S.; Avouris, Ph. *Phys. Rev. Lett.* **2002**, *89*, 126801.
- (7) Dekker: C. *Phys. Today* **1999**, *52*, 22–28.
- (8) Kong, J.; Soh, H. T.; Cassell, A. M.; Quate, C. F.; Dai, H. *Nature* **1998**, *395*, 878. Wind, S. J.; Martel, R.; Avouris, Ph. *J. Vac. Sci. Technol., B* **2002**, *20*, 2745–2748.
- (9) Marty, L.; Bouchiat, V.; Bonnot, A. M.; Chaumont, M.; Fournier, T.; Decossas, S.; Roche, S. *Microelectron. Eng.* **2002**, *61–62*, 485.
- (10) Franklin, N. R.; Wang, Q.; Tomblor, T. W.; Javey, A.; Shim, M.; Dai, H. *Appl. Phys. Lett.* **2002**, *81*, 913–915.
- (11) Diehl, M. R.; Yaliraki S. N.; Beckman, R. A.; Barahona, M.; Heath J. R. *Angew. Chem., Int. Ed.* **2002**, *41*, 353. Valentin, E.; Auvray, S.; Goethals, J.; Lewenstein, J.; Capes, L.; Filoramo, A.; Ribayrol, A.; Tsui, R.; Bourgoin, J.-P.; Patillon, J. N. *Microelectron. Eng.* **2002**, *61*, 491.
- (12) Qi, P.; Vermesh, O.; Grecu, M.; Javey, A.; Wang, Q.; Dai, H.; Peng, S.; Cho, K. J. *Nano Lett.* **2003**, *3*, 347.
- (13) Bonnot, A. M.; Mathis, B. S.; Moulin, S. *Appl. Phys. Lett.* **1993**, *63*, 1754.
- (14) Marty, L.; Naud, C.; Bouchiat, V.; Roche, S.; Chaumont, M.; Fournier, T.; Bonnot, A. M. *Phys. Rev. Lett.*, submitted for publication.
- (15) Martel, R.; Derycke, V.; Lavoie, C.; Appenzeller, J.; Chan, K. K.; Tersoff, J.; Avouris, Ph. *Phys. Rev. Lett.* **2001**, *87*, 256805.
- (16) Zhang, Y.; Ichihashi, T.; Landree, E.; Nihey, F.; Iijima, S. *Science* **1999**, *285*, 1719–1722.
- (17) Lu, K. L.; Lago, R. M.; Chen, Y. K.; Green, M. L. H.; Harris, P. J. F.; Tsang, S. C. *Carbon* **1996**, *34*, 814. Wong, S. S.; Joselevich, E.; Woolley, A. T.; Cheung, C. L.; Lieber, C. M. *Nature* **1998**, *394*, 52.
- (18) Collins, P. G.; Arnold, M. S.; Avouris, Ph. *Science* **2001**, *292*, 706.
- (19) Derycke, V.; Martel, R.; Appenzeller, J.; Avouris, Ph. *Appl. Phys. Lett.* **2002**, *80*, 2773.
- (20) Babic, B.; Iqbal, M.; Schönerberger, C. *Nanotechnology* **2003**, *14*, 327.
- (21) Cui, J. B.; Sordan, R.; Burghard, M.; Kern, K. *Appl. Phys. Lett.* **2002**, *81*, 3260.
- (22) Radosavljevic, M.; Freitag, M.; Thadani, K. V.; Johnson, A. T. *Nano Lett.* **2002**, *2*, 761.
- (23) Fuhrer, M. S.; Kim, B. M.; Dürkop, T.; Britlinger, T. *Nano Lett.* **2002**, *2*, 755.
- (24) Kim, W.; Javey, A.; Vermesch, O.; Wiang, Q.; Li, Y.; Dai, H. *Nano Lett.* **2003**, *3*, 193.
- (25) Yoneya, N.; Tsukagoshi, K.; Aoyagi, Y. *Appl. Phys. Lett.* **2002**, *81*, 2250.
- (26) Katz, H. E.; Hong, X. M.; Dodabalapur, A.; Sarpeshkar, R. *J. Appl. Phys.* **2002**, *91*, 1572.
- (27) Vanheusden, K.; Warren, W. L.; Devine, R. A. B.; Fleetwood, D. M.; Schwank, J. R.; Shaneyfelt, M. R.; Winokur, P. S.; Lemnios, Z. *J. Nature* **1997**, *386*, 587.
- (28) Yano, K.; Ishii, T.; Sano, T.; Mine, T.; Murai, F.; Hashimoto, T.; Kobayashi, T.; Kure, T.; Seki, K. *Proc. IEEE* **1999**, *87*, nr4.
- (29) Futatsugi, T.; Nakajima, A.; Nakao, H. *Fujitsu Sci. Tech. J.* **1998**, *34*, 142.
- (30) Cui, J. B.; Burghard, M.; Kern, K. *Nano Lett.* **2002**, *2*, 117.
- (31) Woodside, M. T.; McEuen, P. L. *Science* **2002**, *296*, 1098.
- (32) Ruzin, I. M.; Chandrasekhar, V.; Levin, E. I.; Glazman, L. I. *Phys. Rev. B* **1992**, *45*, 13469.
- (33) Tans, S. J.; Devoret, M. H.; Dai, H.; Thess, A.; Smalley, R. E.; Geerligs, L. J.; Dekker, C. *Nature* **1997**, *386*, 474.
- (34) Smith, R. A.; Ahmed, H. *J. Appl. Phys.* **1997**, *81*, 2699.
- (35) Evans, G. J.; Mizuta, H.; Ahmed, H. *Jpn. J. Appl. Phys.* **2001**, *40*, 5837.
- (36) Freitag, M.; Johnson, A. T.; Kalinin, S. V.; Bonnell, D. A. *Phys. Rev. Lett.* **2002**, *89*, 216801.
- (37) Sato, T.; Ahmed, H.; Brown, D.; Johnson, B. F. G. *J. Appl. Phys.* **1997**, *82*, 696.

NL0342848